An Adaptive Neuro-Fuzzy Inference Approach of AOA/AOS Data Fusion for Small Fixed-Wing UAV

Bowen Duan[1,†][a], Yiming Wang[1,†][b], Heng Wang[1,†][c], Yunxiao Liu[1,†][d], Han Li[2,†][e] and Jianliang Ai[1,*][f]

[1]*Department of Aeronautics & Astronautics, Fudan University, 220 Handan Road, Shanghai 200433, China*

[2]*Department of Electrical Engineering, University of Shanghai for Science and Technology, 516 Jungong Road, Shanghai 200093, China*

{*bwduan21, yimingwang23, hengwang21*}*@m.fudan.edu.cn, yunxiaoliu20@fudan.edu.cn, hanli@usst.edu.cn,*

Keywords: Angle of Attack, Angle of Sideslip, Small-Sized UAV, Data Fusion, Adaptive Network-Based Fuzzy Inference System.

Abstract: Accurate measurement of angle of attack (AOA) and angle of sideslip (AOS) is crucial for ensuring the safe operation of fixed-wing unmanned aerial vehicles (UAVs) and conducting reliable flight performance evaluations. Given the limited payload capacity of small-sized UAVs, lightweight wind vane probes are commonly employed. Although installing wind vane sensors at the nose typically yields accurate measurements, this placement is impractical for UAVs with front-mounted propellers. An alternative is to position the sensors beneath the wing, but this configuration introduces measurement inaccuracies due to propeller-induced slipstream and fuselage obstruction. To address these challenges, estimating AOA and AOS using inertial data through the unscented Kalman filter (UKF) offers a more robust solution, as it is less affected by external disturbances. This study introduces an adaptive network-based fuzzy inference system (ANFIS) for AOA/AOS data fusion, which compensates for inaccuracies in sensor measurements by integrating UKF-estimated AOA and AOS values. Flight test results demonstrate that the proposed ANFIS model achieves an average relative error of less than 15 %, with the average relative errors being 10.26 % for AOA and 12.77 % for AOS. This fusion approach significantly enhances the accuracy of AOA and AOS measurements, providing a valuable reference for small-sized fixed-wing UAVs.

1 INTRODUCTION

The angle of attack (AOA) and angle of slip (AOS) are important parameters affecting fixed-wing unmanned aerial vehicles (UAVs) aerodynamics. Therefore, accurate measurement of AOA and AOS is necessary for ensuring the safe flight of fixed-wing UAVs and achieving flight performance evaluation (Sankaralingam and Ramprasadh, 2020). Small fixed-wing UAVs with a take-off weight of less than 10 kg have the unique mission advantage of being portable and easy to deploy. They have been widely used in surveying and mapping, surveillance, meteorological monitoring, and other fields (Wang et al., 2023).

Standard AOA/AOS measure methods mainly include the wind vane probe sensor measurement method, multi-hole probe sensor measurement method, and data fusion estimation method. Due to the limited payload weight of small fixed-wing UAVs, wind vane probes are the more commonly used AOA/AOS measurement sensors (Data, 2024; Prem et al., 2020). This type of sensor has the advantage of lightweight, simple, and reliable measurement principles. However, measurement failures may be caused by hardware installation positions or sensor failures when deployed in UAVs. In order to overcome those problems, various improvement methods have been proposed, mainly including flow angle estimation filters and redundant measurement methods

[a] https://orcid.org/0009-0004-1101-3744
[b] https://orcid.org/0009-0002-5100-977X
[c] https://orcid.org/0009-0003-5207-6832
[d] https://orcid.org/0009-0004-0593-9444
[e] https://orcid.org/0009-0007-0284-2083
[f] https://orcid.org/0000-0002-8982-8503

† means these authors contributed equally to this work and should be considered co-first authors; * means the corresponding author.

Duan, B., Wang, Y., Wang, H., Liu, Y., Li, H. and Ai, J.
An Adaptive Neuro-Fuzzy Inference Approach of AOA/AOS Data Fusion for Small Fixed-Wing UAV.
DOI: 10.5220/0013431700003929

In *Proceedings of the 27th International Conference on Enterprise Information Systems (ICEIS 2025) - Volume 1*, pages 905-912
ISBN: 978-989-758-749-8; ISSN: 2184-4992

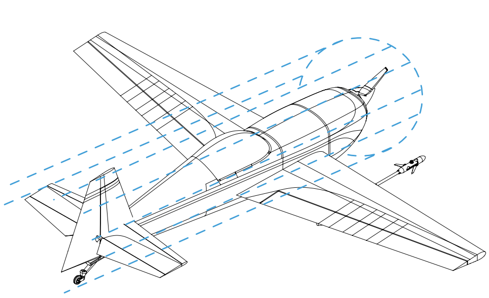

(a) Effect of the propeller induced slipstream;.

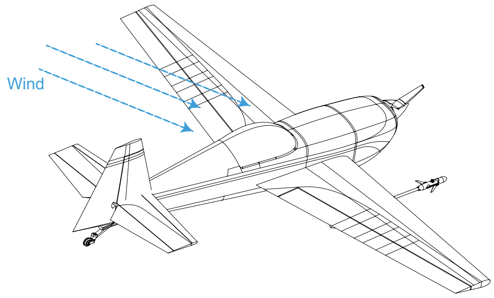

(b) Obstruction caused by the fuselage.

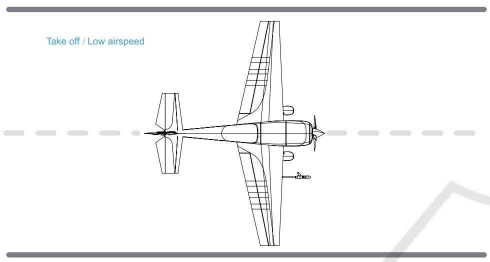

(c) Specific starting torque of the wind vane.

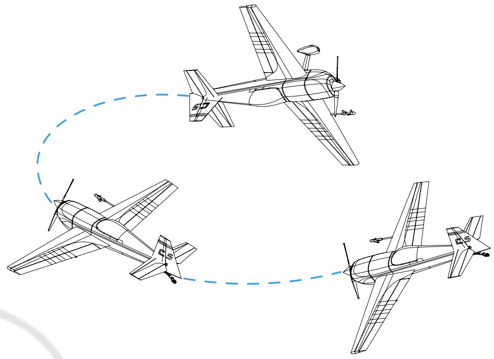

(d) Rapid changes in airflow.

Figure 1: Factors influencing the accuracy of AOA/AOS sensor measurements.

combining wind vane sensors and angle estimation. The flow angle estimation filters method is based on the measured UAV airspeed, acceleration, and attitude angle for fusion estimation. Complementary filters (Myschik et al., 2008), Kalman filters (Johansen et al., 2015; Wenz et al., 2016), and extended Kalman filters (Rhudy et al., 2013; Tian et al., 2018), etc. have been proposed. The advantage of this method is that it can realize AOA/AOS estimation without a flow angle sensor, but there may be inevitable calculation delays when applied. Regarding engineering applications, a redundant measurement method was proposed to improve the above method, combining wind vane sensors and angle estimation (Liu et al., 2024). This method uses an onboard computer to process the wind vane sensor measurement data and realizes accurate estimation of AOA/AOS based on the unscented Kalman filter (UKF). The robustness of AOA/AOS measurement during UAV flight is improved based on the real-time analysis and calculation of the two data.

The above methods and results benefit the application of AOA/AOS on small fixed-wing UAVs. However, there are still several key issues that may affect the measurement accuracy in engineering applications: (1) For UAVs with front-mounted propellers, the influence of propeller slipstream cannot be avoided entirely when the sensor is installed on the UAV fuselage; (2) Due to the installation position of the sensor, when the UAV is in a hovering maneuvering state, the fuselage obstruction may affect the accurate measurement of AOS; (3) Since the rotation of the wind vane requires a specific starting torque when the UAV is taxiing and flying at low speed, the AOA/AOS measurement may fail; (4) When the UAV performs continuous dynamic maneuvering flight, the dynamic overshoot and oscillation of the wind vane may occur due to the rapid change of airflow. The specific scenarios illustrated in (1) to (4) are shown in Fig. 1.

The key to solving these problems is researching the error generation mechanism of wind vane probes in small fixed-wing UAV applications and implementing the perception, decision, and error correction of the AOA/AOS measurement process based on multi-condition process monitoring and fusion decision algorithms. Among them, a potential solution is to implement condition labeling for problems (1) to (4) and design a dynamic adjustment mechanism for error correction of wind vane sensor and angle estimation redundant measurement method based on fusion decision algorithms, thereby eliminating the hardware measurement defects of wind vane sensors and further improving the measurement accuracy of redundant measurement methods in applications.

The main contribution of this paper could be categorized into three aspects: (1) Motivated by (Liu et al., 2024), a novel measurement method was developed for small fixed-wing UAVs, integrating data acquisition using wind vane-based sensors with estimation via the UKF algorithm; (2) For small fixed-wing UAVs equipped with front-mounted propellers, a detailed analysis was conducted to identify potential factors impacting the measurement accuracy of sensors installed beneath the wing; (3) To address inaccuracies in sensor measurements, an AOA/AOS fusion method based on the adaptive network-based fuzzy inference system (ANFIS) was proposed, leveraging UKF-estimated values for compensation.

The remainder of this paper is structured as follows: Section 2 presents the design of the wind vane-based sensor and the UKF-based AOA/AOS estimation method. Section 3 investigates potential factors influencing the measurement accuracy of sensors mounted beneath the wing and proposes an AOA/AOS fusion method utilizing ANFIS. Section 4 presents the flight test conducted for data collection and the simulation experiments designed to validate the proposed data fusion approach. Finally, Section 5 provides a comprehensive summary of the study.

2 PRELIMINARY

Two approaches are available for recording AOA and AOS. The first involves using the low-cost wind vane-based AOA and AOS sensors. The second relies on estimating AOA and AOS through the UKF algorithm from inertial data.

2.1 Low-Cost AOA/AOS Sensors

A set of AOA and AOS sensors based on the rotation of wind vane blades was employed to measure the α and β angle (also known as AOA and AOS) during the flight. The sensor housing features a streamlined design and is fabricated using 3D printing with aluminum alloy. Inside the sensor, two brushless Hall magnetic angle sensors are positioned perpendicular to one another at a 90°. Two carbon fiber wind vane blades are affixed to the rotational axes of these sensors, respectively. Additionally, a balancing block is mounted on the symmetrical side of the wind vane to ensure weight balance. The total weight of the sensor assembly is approximately 25 g, with an encoder resolution of 0.088°.

When subjected to the incoming flow, the wind vane blades drive the rotational axes of the angle sensors. The phase and intensity of the rotational magnetic field are detected by monitoring the Hall element array, enabling the measured values of the α and β to be converted into digital signals and directly output via I2C communication. To mitigate high-frequency noise resulting from engine vibration, structure vibration, and mechanical nonlinearity during sensor installation, the collected data are filtered using the finite impulse response (FIR) method (Sulaiman et al., 2022).

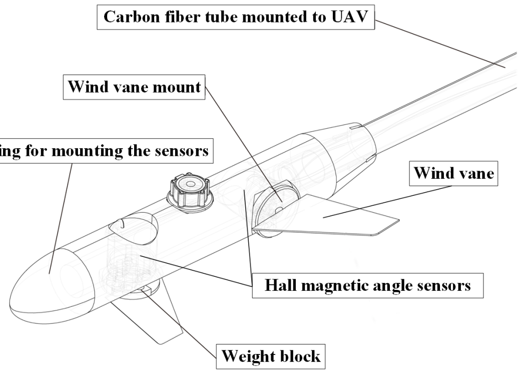

Figure 2: Structure of AOA/AOS sensors.

The sensor is connected to the UAV via a mounting carbon tube that passes through the structural housing. For UAVs with rear-mounted propellers, the sensor can be installed on the nose of the UAV, providing direct access to undisturbed free airflow. This positioning helps avoid the effects of propeller-induced airflow disturbances, thereby ensuring high data measurement accuracy. However, for UAVs with front-mounted propellers, the nose position becomes unsuitable for sensor installation.

A feasible solution is to install the sensor beneath one side of the wing, as illustrated in Fig. 3b. However, due to airflow disturbances caused by the propeller and obstruction from the fuselage, this installation position inevitably affects the sensor's measurements and may even result in missing data.

2.2 AOA/AOS Estimation Method

In addition to the measurement from the AOA and AOS sensors, the α and β can be estimated by fusing inertial data collected by the flight controller. This estimation process remains unaffected by the operational status of AOA/AOS sensors, making it a reliable and effective redundancy solution.

As an improvement of the extended Kalman filter, the UKF offers superior accuracy for nonlinear distribution statistics (Julier and Uhlmann, 1997). In this paper, an estimation method based on the UKF was adopted to estimate α and β using the inertial data. The state estimation model for predicting the state at

(a) At the nose;.

(b) Beneath the wing.

Figure 3: Two different installation configurations.

time step k using the state at time step $k-1$ is defined as:

$$\begin{cases} \mathbf{X}_k = f\left(\mathbf{X}_{k-1}, \mathbf{u}_{k-1}\right) + \mathbf{w}_{k-1} \\ \mathbf{Z}_k = h\left(\mathbf{X}_k, \mathbf{u}_k\right) + \mathbf{v}_k \end{cases} \tag{1}$$

where $\mathbf{w}$ and $\mathbf{v}$ are the process and measurement noise, respectively; the state vector $\mathbf{X}$, the measurement vector $\mathbf{Z}$, and input vector $\mathbf{u}$ is defined as:

$$\begin{aligned} \mathbf{X} &= [\alpha, \beta] \\ \mathbf{Z} &= [\alpha, \beta] \\ \mathbf{u} &= [a_x, a_y, a_z, p, q, r, \theta, \phi, V] \end{aligned} \tag{2}$$

where $[a_x, a_y, a_z]$ represents the three-axis acceleration; $[p, q, r]$ represents the three-axis angular velocity; θ and ϕ represent the pitch and roll angle, respectively; and V represents the airspeed.

The state transition equation $f(\cdot)$ is:

$$\begin{cases} \dot{\alpha} = \dfrac{1}{mV\cos\beta}[-T\sin\alpha + mV(-p\cos\alpha\sin\beta + \\ q\cos\beta - r\sin\alpha\sin\beta) + mg(\sin\alpha\sin\theta + \\ \cos\alpha\cos\phi\cos\theta) - L] \\ \dot{\beta} = \dfrac{1}{mV}[-T\cos\alpha\sin\beta + Y - mV(-p\sin\alpha + \\ r\cos\alpha) + mg(\cos\alpha\sin\beta\sin\theta + \cos\beta\sin\phi\cos\theta - \\ \sin\alpha\sin\beta\cos\phi\cos\theta) \end{cases} \tag{3}$$

where m represents the mass of the UAV; T, L, and Y represent the thrust, lift, and side force of the UAV, respectively.

The measurement vector $\mathbf{Z}$ is obtained using the nonlinear measurement function $f(\cdot)$, which is defined as:

$$\mathbf{Z} = h(\mathbf{X}, \mathbf{u}, \mathbf{v}) = \\ \begin{bmatrix} \frac{1}{C_{L\alpha}}\left(\frac{m(a_x\sin\alpha - a_z\cos\alpha) - T\sin\alpha}{\frac{1}{2}\rho V^2 S} - C_{L_0} - C_{L_q}\frac{b}{2V}q - C_{L_{\delta_e}}\delta_e\right) \\ \frac{1}{C_{Y_\beta}}\left(\frac{2ma_y}{\rho V^2 S} - C_{Y_0} - C_{Y_p}\frac{b}{2V}p - C_{Y_r}\frac{b}{2V}r - C_{Y_{\delta_a}}\delta_a - C_{Y_{\delta_r}}\delta_r\right) \end{bmatrix} \tag{4}$$

where ρ is the atmospheric density at sea level; b denotes the wing span; S denotes the wing area; C_{L_*} and C_{Y_*} represent the lift and side force coefficients associated with the parameter $*$ respectively.

3 METHOD

For small-sized UAVs with front-mounted propellers, installing sensors beneath the wing is a practical choice. However, this positioning inevitably compromises measurement accuracy. To mitigate this issue, we proposed an ANFIS-based AOA/AOS data fusion framework that leverages UKF-estimated values to correct inaccuracies in sensor measurements.

3.1 Impact Factor Selection

In engineering applications, the precision of angle sensors is often affected by many complex factors. These elements encompass the flight conditions of the UAV, the physical characteristics of sensors, and their positioning during installation. The effects of these factors on measurement accuracy are interconnected and cannot be clearly expressed in mathematical formulas, which augment the intricacy of the measurement system.

To better understand and address these impact factors, this study abstracts them into three key physical quantities, airspeed, yaw angle, and sensor status, that can be measured and used as inputs to the ANFIS estimation model. Each of these factors affects the AOA and AOS measurements through distinct mechanisms.

Airspeed is a crucial factor impacting sensor accuracy. It is generally accepted that the AOA/AOS sensor typically has a minimum operational airspeed of $10\,\mathrm{m/s}$. If the airspeed falls below this threshold, the sensor either fails to activate or produces unreliable measurements. Also, if the airspeed is too high, rapid airflow changes may cause the wind vane to overshoot or oscillate, thereby reducing measurement accuracy.

Flight yaw angle variations typically occur during UAV maneuvers, such as turns or spirals. In these

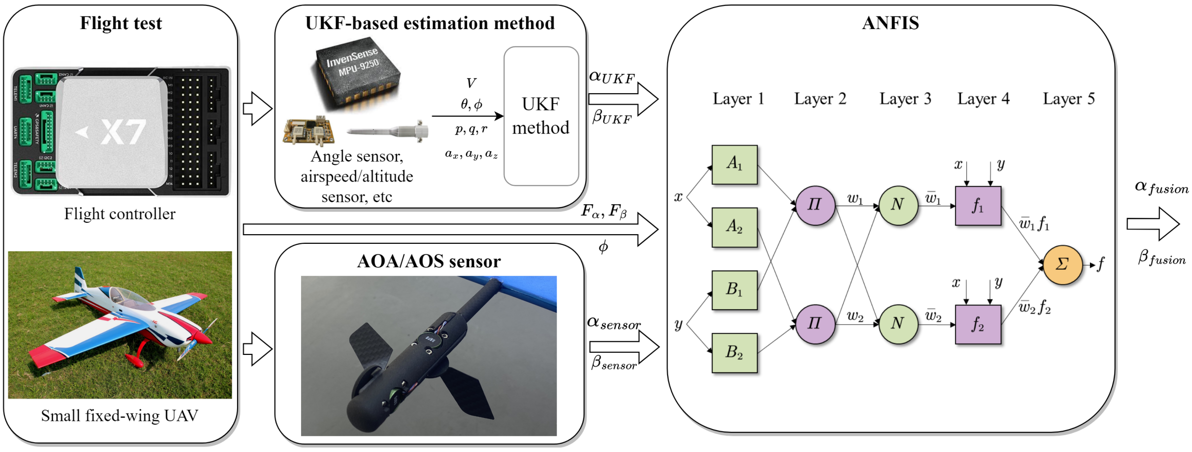

Figure 4: ANFIS-based AOA/AOS fusion approach.

cases, due to the fuselage's blocking effect, the sensor cannot be able to accurately detect the direction and speed of airflow, especially leading to errors in AOS measurements. By continuously monitoring the flight yaw angle, these errors can be identified and corrected in real-time, improving the accuracy of angle measurements.

Sensor malfunctions, in this study, were categorized into two types: null value faults (denoted as 1) and extreme value faults (denoted as 2). Extreme value faults typically occur when AOA exceeds $\pm 20^\circ$ or AOS exceeds $\pm 60^\circ$, while null value faults indicate that the sensor fails to provide valid data, often returning a NaN. In such cases, the reliability of the sensor's data is compromised. The sensor is expected to provide relatively valid measurement data only when it is in a normal operating state (denoted as 0).

In designing the ANFIS model based on actual flight data, the three key factors mentioned above, airspeed, yaw angle, and sensor malfunction type, along with the sensor's output and the estimation from the UKF algorithm, are utilized as inputs to the ANFIS system. This approach enables the simulation of various error sources present in real measurement scenarios and makes full use of prior knowledge to enhance the accuracy of AOA and AOS measurements.

3.2 AOA/AOS Fusion Method

Considering the interference effects analyzed above, we proposed a novel data fusion approach based on the ANFIS. This approach utilizes the UKF-estimated AOA and AOS to compensate for the AOA/AOS sensor measurements affected by the disturbances.

As a combination of fuzzy logic and artificial neural networks, ANFIS combines the learning ability and relational structure of the artificial neural networks with the fuzzy logic's decision-making mechanism (Jang, 1993). Benefiting from the fuzzy inference system embedded in its network structure, ANFIS effectively addresses the issue of non-interpretable weight values commonly found in other artificial neural networks. As a result, it has been extensively utilized in addressing a wide range of complex problems (Karaboga and Kaya, 2019; Guerra et al., 2024).

To facilitate understanding of its principle, consider a case where ANFIS has two inputs (x, y) and one output f. Notably, it can be readily generalized to scenarios involving more inputs. The network structure of ANFIS comprises five layers.

The first layer, known as the fuzzification layer, transforms the input values (x, y) into fuzzy clusters defined by Gaussian membership functions, which can be expressed as:

$$\begin{cases} Q_i^1 = \mu_{A_i}(x) & i = 1,2 \\ Q_i^1 = \mu_{B_{i-2}}(x) & i = 3,4 \end{cases} \tag{5}$$

where Q_i^1 represents the membership grades of node i in the fuzzification layer; $\mu_{A_i}(\cdot)$ and $\mu_{B_{i-2}}(\cdot)$ represent Gaussian membership functions of x in the corresponding fuzzy cluster, which is:

$$\mu_k(x) = \exp\left(-\frac{(x - c_k)^2}{2\sigma_k^2}\right) \tag{6}$$

where c_k is the center of the Gaussian function, and σ_k is the standard deviation that controls the width of the cluster.

The second layer, referred to as the rule layer, computes the firing strengths w_i of the rules by multiplying the membership grade values obtained in the fuzzification layer:

$$O_i^2 = w_i = \mu_{A_i}(x) \cdot \mu_{B_{i-2}}(x) \quad i = 1,2 \tag{7}$$

The third layer, referred to as the normalization layer, scales the firing strengths of each rule to ensure proportional consistency. The normalized value for the i-th rule is:

$$O_i^3 = \bar{w}_i = \frac{w_i}{\sum_j^4 w_j} \quad i \in 1,2,3,4 \tag{8}$$

The fourth layer, referred to as the defuzzification layer, calculates the weighted value of each rule at each node. This value is determined by a first-order polynomial:

$$O_i^4 = \bar{w}_i f_i = \bar{w}_i \left(p_i x + q_i y + r_i\right) \quad i \in 1,2,3,4 \tag{9}$$

where (p_i, q_i, r_i) is called the consequence parameters. The dimension of consequence parameters is one more than that of input states.

The fifth layer, known as the summation layer, generates the final output by summing the weighted values calculated in the defuzzification layer:

$$O_i^5 = \sum_i \bar{w}_i f_i = \frac{\sum_i w_i f_i}{\sum_i w_i} \tag{10}$$

The training algorithm employed in this paper utilizes a hybrid method that combines two distinct optimization techniques: backpropagation for optimizing the parameters associated with the input membership functions and least squares estimation for optimizing the parameters associated with the output membership functions.

4 EXPERIMENTS AND RESULT

The small fixed-wing UAV used in the flight test was EXTRA 300 NG, with its specification available in (Liu et al., 2024). The AOA/AOS sensors were installed on the right wing because of its forward propeller. A CUAV X7+ flight controller on the UAV platform collects data from the IMU, GPS, electronic compass, airspeed sensor, and other units. Specifically, an onboard Raspberry Pi recorded the AOA and AOS during the flight.

The flight test lasted approximately 2 min. During this period, the UAV followed pre-defined waypoints, automatically performing climbing, cruising, maneuvering, and descent. $[a_x, a_y, a_z]$, $[p, q, r]$, $[\psi, \theta, \phi]$, $[\delta_a, \delta_e, \delta_r]$, and V were recorded using the CUAV X7+ flight controller, while α and β were recorded by the AOA/AOS sensor on the right wing. The flight test trajectory is illustrated in Fig. 5.

In this paper, the ANFIS was employed by Matlab R2024a. The computer configuration employed includes a 12th Gen Intel(R) Core(TM) i9-12900H processor running on a Windows 11 operating system. The approach is shown in Fig. 4.

AOA and AOS were treated separately, with a corresponding ANFIS developed for each angle. Taking

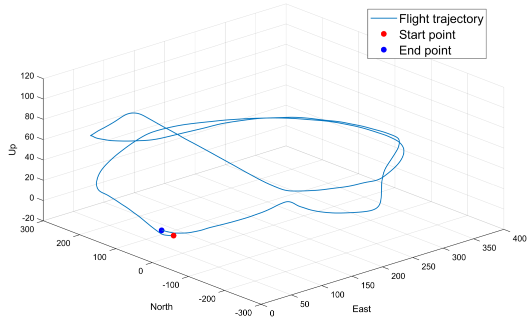

(a) Three-dimensional flight trajectory;.

(b) Two-dimensional plane trajectory.

Figure 5: Flight test trajectory.

AOA as an example, the inputs to the network are the AOA sensor measurement $\hat{\alpha}_{\text{sensor}}$, the AOA estimate from UKF $\hat{\alpha}_{\text{UKF}}$, airspeed V, the yaw angle ψ, the fault type of AOA sensor F_α; and the output is the actual value of AOA. Each input variable is associated with eleven Gaussian membership functions, and the output layer employs a linear relationship, where the outputs from all fuzzy sets are aggregated through weighted summation to produce the final prediction.

70 % of the data were randomly sampled from the original dataset and designated as the training set. After normalization, the data was fed into the ANFIS. The error tolerance was set to 10^{-8}, and the epochs were set to 300.

As illustrated in Fig. 6 and Fig. 7, comparisons of the fusion values of ANFIS with the actual values are demonstrated for both AOA and AOS testing sets. Table 1 provides a statistical analysis.

Table 1: Statistical analysis of ANFIS fusion results.

	AOA	**AOS**
Average Relative Error	10.26 %	12.77 %
Root Mean Square Error	0.652°	0.542°
Correlation Coefficient	0.912	0.891

The performance of ANFIS data fusion for the AOA and AOS of the selected UAVs was evaluated using test datasets. The results indicate that ANFIS can effectively predict the actual values by integrating

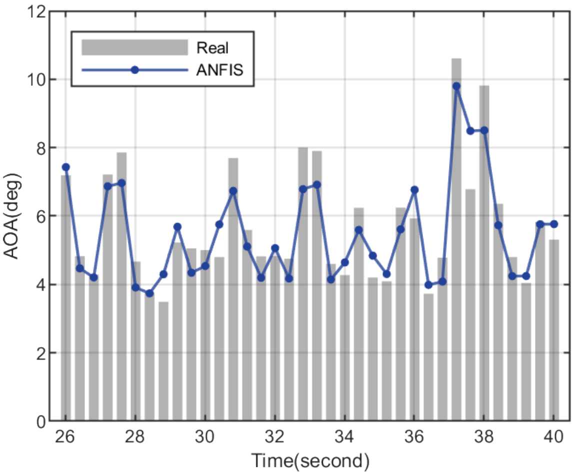

Figure 6: Fusion results of AOA.

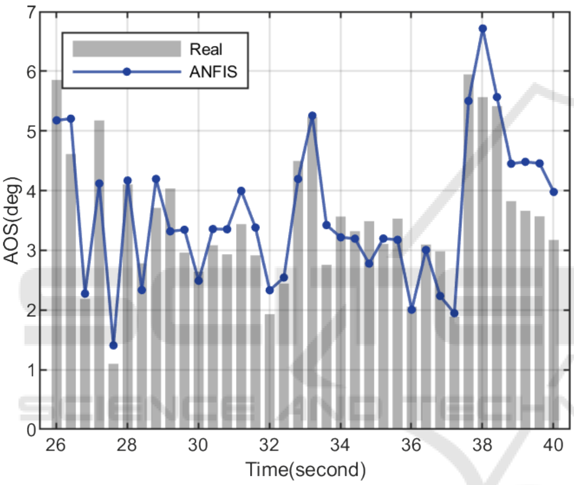

Figure 7: Fusion results of AOS.

sensor measurements and UKF estimates, taking into account various influencing factors. The average relative error between the predicted and actual values of the ANFIS model proposed in this paper is less than 15 %, with the average relative errors being 10.26 % for AOA and 12.77 % for AOS. These results demonstrate that the proposed method can effectively incorporate prior knowledge and account for the influencing factors, thus providing accurate fusion results that meet the application requirements.

5 CONCLUSION

This paper proposes a novel and intelligent error correction method for wind sensors measuring AOA and AOS in small fixed-wing UAVs. The proposed method utilizes the ANFIS framework. The study identifies the main measurement error sources as sensor null/extreme faults, airframe occlusion, and too low/too high airspeed. The proposed mechanism employs an adaptive correction process to address system faults by leveraging actual sensor measurements, UKF estimates, and error sources to generate more precise angle fusion results. Numerical experiments demonstrate that the system employing this architecture effectively mitigates the hardware measurement defects of the wind vane sensor, with an average relative error of less than 15 %, which falls within the acceptable margin.

In future research, we plan to include more complex sensor failure scenarios. Furthermore, the study will investigate real-time dynamic tuning algorithms to improve the measurement accuracy of redundant measurement methods for small UAVs.

REFERENCES

Data, S. A. (Accessed: 24-Dec-2024). Smv-1 flow vane. Online: https://www.swiss-airdata.com/products/flow-vanes/smv-1.

Guerra, M. I., de Araújo, F. M., de Carvalho Neto, J. T., and Vieira, R. G. (2024). Survey on adaptative neural fuzzy inference system (anfis) architecture applied to photovoltaic systems. *Energy Systems*, 15(2):505–541.

Jang, J.-S. (1993). Anfis: adaptive-network-based fuzzy inference system. *IEEE transactions on systems, man, and cybernetics*, 23(3):665–685.

Johansen, T. A., Cristofaro, A., Sørensen, K., Hansen, J. M., and Fossen, T. I. (2015). On estimation of wind velocity, angle-of-attack and sideslip angle of small uavs using standard sensors. In *2015 International Conference on Unmanned Aircraft Systems (ICUAS)*, pages 510–519. IEEE.

Julier, S. J. and Uhlmann, J. K. (1997). New extension of the kalman filter to nonlinear systems. In *Signal processing, sensor fusion, and target recognition VI*, volume 3068, pages 182–193. Spie.

Karaboga, D. and Kaya, E. (2019). Adaptive network based fuzzy inference system (anfis) training approaches: a comprehensive survey. *Artificial Intelligence Review*, 52(4):2263–2293.

Liu, Y., Wang, Y., Wang, L., Li, H., and Ai, J. (2024). Development of a low-cost aoa/aos sensor and data processing system for small-sized uavs. In *2024 IEEE 19th Conference on Industrial Electronics and Applications (ICIEA)*, pages 1–6. IEEE.

Myschik, S., Holzapfel, F., and Sachs, G. (2008). Low-cost sensor based integrated airdata and navigation system for general aviation aircraft. In *AIAA Guidance, Navigation and Control Conference and Exhibit*, page 7423.

Prem, S., Sankaralingam, L., and Ramprasadh, C. (2020). Pseudomeasurement-aided estimation of angle of attack in mini unmanned aerial vehicle. *Journal of Aerospace Information Systems*, 17(11):603–614.

Rhudy, M. B., Larrabee, T., Chao, H., Gu, Y., and Napolitano, M. (2013). Uav attitude, heading, and wind estimation using gps/ins and an air data system. In *AIAA guidance, navigation, and control (GNC) conference*, page 5201.

Sankaralingam, L. and Ramprasadh, C. (2020). A comprehensive survey on the methods of angle of attack measurement and estimation in uavs. *Chinese Journal of Aeronautics*, 33(3):749–770.

Sulaiman, I. A., Hassan, H. M., Danish, M., Singh, M., Singh, P., and Rajoriya, M. (2022). Design, comparison and analysis of low pass fir filter using window techniques method. *Materials Today: Proceedings*, 49:3117–3121.

Tian, P., Chao, H., Flanagan, H. P., Hagerott, S. G., and Gu, Y. (2018). Design and evaluation of uav flow angle estimation filters. *IEEE Transactions on Aerospace and Electronic Systems*, 55(1):371–383.

Wang, L., Li, H., Liu, Y., and Ai, J. (2023). Design and realization of a cable-drogue aerial recharging device for small electric fixed-wing uavs. In *2023 International Conference on Unmanned Aircraft Systems (ICUAS)*, pages 926–932. IEEE.

Wenz, A., Johansen, T. A., and Cristofaro, A. (2016). Combining model-free and model-based angle of attack estimation for small fixed-wing uavs using a standard sensor suite. In *2016 International Conference on Unmanned Aircraft Systems (ICUAS)*, pages 624–632. IEEE.